Molecular Crystals and Liquid Crystals
Publication details, including instructions for authors and subscription information:
http://www.informaworld.com/smpp/title~content=t713644168

Synthesis and Hole Transport Properties of Highly Soluble Pyrene-Based Discotic Liquid Crystals with Trialkylsilylethynyl Groups

Takuji Hirose[a]; Yuki Shibano[a]; Yutaro Miyazaki[a]; Norihito Sogoshi[a]; Seiichiro Nakabayashi[a]; Mikio Yasutake[a]
[a] Graduate School of Science and Engineering, Saitama University, Sakura, Saitama, Japan

First published on: 18 January 2011

To cite this Article Hirose, Takuji , Shibano, Yuki , Miyazaki, Yutaro , Sogoshi, Norihito , Nakabayashi, Seiichiro and Yasutake, Mikio(2011) 'Synthesis and Hole Transport Properties of Highly Soluble Pyrene-Based Discotic Liquid Crystals with Trialkylsilylethynyl Groups', Molecular Crystals and Liquid Crystals, 534: 1, 81 — 92
To link to this Article: DOI: 10.1080/15421406.2011.536485
URL: http://dx.doi.org/10.1080/15421406.2011.536485

Mol. Cryst. Liq. Cryst., Vol. 534: pp. 81–92, 2011

ISSN: 1542-1406 print/1563-5287 online
DOI: 10.1080/15421406.2011.536485

Taylor & Francis
Taylor & Francis Group

Synthesis and Hole Transport Properties of Highly Soluble Pyrene-Based Discotic Liquid Crystals with Trialkylsilylethynyl Groups

TAKUJI HIROSE, YUKI SHIBANO, YUTARO MIYAZAKI, NORIHITO SOGOSHI, SEIICHIRO NAKABAYASHI, AND MIKIO YASUTAKE

Graduate School of Science and Engineering, Saitama University, Sakura, Saitama, Japan

Four pyrene-based discotic compounds with trialkylsilylethynyl groups in the side chains were prepared and characterized by differential scanning calorimetry, polarizing optical microscopy, and X-ray diffraction measurements. All of the compounds were highly soluble in organic solvents, and two of the compounds exhibited a columnar phase, Col_r, and the others were crystalline. The hole transport ability in the liquid-crystalline phases was determined by the time-of-flight (TOF) method to be on the order of 10^{-2} cm^2 V^{-1} s^{-1}, the highest hole mobilities for pyrene derivatives yet observed.

Keywords Discotic liquid crystal; hole transport; pyrene derivatives; synthesis; trialkylsilylethynyl group

Introduction

Recently, organic semiconductors have received increasing attention because of their potential applications in organic light-emitting diodes (OLEDs) [1], organic field-effect transistors (OFETs) [2], and so on [3]. Flexible, lightweight, and low-cost electronic devices are expected from organic conductive materials; in fact, some pentacene derivatives are found to have higher charge mobilities than amorphous silicon FETs [4]. However, crystalline organic semiconductors, such as polyacenes, typically have low solubility in organic solvents and expensive high-vacuum deposition is necessary for thin-film preparation in device processing [5]. On the other hand, amorphous organic materials, such as those used in photocopiers and laser printers, have charge mobilities of only 10^{-6}–10^{-5} cm^2 V^{-1} s^{-1}, and therefore their performance is not sufficient for OLEDs and OFETs [6].

In liquid-crystalline semiconductors, problems with processing and the decrease in charge mobilities at the grain boundary are expected to become irrelevant [7]. Therefore, an appropriate molecular design is of great interest and importance for

Address correspondence to Takuji Hirose, Graduate School of Science and Engineering, Saitama University, 255 Shimo-ohkubo, Sakura, Saitama 338-8570, Japan. E-mail: hirose@apc.saitama-u.ac.jp

obtaining conductive liquid-crystalline compounds that exceed the performance of amorphous silicons [8]. One-dimensional charge transport through columns of discotic liquid crystals is a fascinating property of OFET and OLED devices, and charge mobilities up to $\sim 1\,cm^2\,V^{-1}\,s^{-1}$ have been reported [9–12].

High solubility in common organic solvents, which would allow the material to be processed in solution, is another requirement [8,13]. We have attempted to develop columnar liquid-crystalline materials with pyrene as a relatively small π-conjugated core in order to obtain high solubility [14]. However, the particular molecular design necessary for high charge mobility remained unclear. It is known that the σ-orbitals of silicon interact strongly with adjacent π-electron systems (σ-π conjugation), thus enhancing the conjugation of the system [15–18]. In addition, it has been reported that introduction of trialkylsilyl groups enhances the solubility of organic compounds and the ability of polymer materials to form films [19]. However, to the best of our knowledge, the electrical properties of liquid-crystalline compounds bearing trialkylsilyl groups have not yet been reported [20]. In this article, we report the synthesis of novel columnar liquid crystals having a pyrene core bearing trialkylsilylethynyl groups as flexible side chains, as well as the hole transport properties of these materials as determined in time-of-flight (TOF) studies.

Experimental

General

^{1}H nuclear magetic resonance (NMR) spectra were recorded on Bruker AC-200, Bruker AC-300P, and Bruker DRX-400 spectrometers (Molecular Analysis and Life Science Center [MALS], Saitama University). The chemical shift was reported in parts per million using tetramethylsilane as an internal standard. Matrix-assisted laser desorption/ionization time-of-flight (MALDI-TOF) mass spectra were measured with a Bruker Daltonics autoflex III (MALS). UV-Vis spectra were recorded as a hexane solution on a JASCO V-550.

Phase transition temperatures were determined using a Mac Science DSC-3100 differential scanning calorimeter (DSC). Polarizing optical microscopy (POM) was performed using a Nikon OPTIPHOT2-POL equipped with a Mettler FP-82 hot stage and a Mettler FP-90 central processor to verify thermal transitions and characterize anisotropic textures. X-ray diffraction (XRD) analysis was performed on quartz substrate using a Rigake model Ultima III X-ray diffractometer with a monochromated CuK_α radiation source.

The carrier transport was characterized using a conventional TOF setup equipped with an Nd:YAG laser ($\lambda = 355$ nm, pulse width = 20 ns, 0.5 mJ pulse^{-1}). A bias voltage was applied across the sample by a dc power supply and the transient photocurrents were monitored with a digital oscilloscope at a given temperature maintained by a homemade hot stage. The transit time for carriers was determined from the shoulder in the transient photocurrent.

The pyrene derivatives were injected into the cell ($l = 5.0$-μm-thick ITO-coated glass cells of 100 mm^2 electrode area) by capillary action, and then the samples were slowly cooled to room temperature from their isotropic temperatures. The applied electric field, E, was 4.4–5.5 kV cm^{-1} for **A5** and 3.0 kV cm^{-1} for **A6** [11,26]. The mobility, μ, was calculated using the relation $\mu = l/(\tau_T \cdot E)$, where τ_T is the transit

time. The POM observation showed birefringent textures for both **A5** and **A6**, indicating the polydomain alignments.

Synthesis

3,5-Bis(trimethylsilylethynyl)bromobenzene 1 [21]. Under nitrogen, $PdCl_2(PPh_3)_2$ (362 mg, 0.516 mmol), PPh_3 (271 mg, 1.03 mmol), *i*-Pr_2NH (10 mL), trimethylsilylacetylene (TMSA); (2.23 g, 22.7 mmol), and CuI (99 mg, 0.52 mmol) were added to 1,3,5-tribromobenzene (3.25 g, 10.3 mmol) in dry THF (30 mL). After stirring at 50°C for 20 h, the reaction mixture was cooled to room temperature and then filtered through Celite. The filtrate was concentrated and the residue was extracted with chloroform and water. The organic layer was dried over anhydrous Na_2SO_4 and concentrated to give a brown liquid. The crude product was purified by silica gel column chromatography with hexane and purified by thin-layer chromatography (TLC) on silica gel with hexane to give a colorless liquid **1** (56.4%, 2.04 g, 5.82 mmol). ^{1}H NMR (300 MHz, $CDCl_3$): δ (ppm) = 0.236 (*s*, 18H, CH_3), 7.49 (*t*, 1H, $J = 1.5$ Hz, Ar-H), 7.53 (*d*, 2H, $J = 1.5$ Hz, Ar-H).

3,5-Diethylbromobenzene 2. To the solution of **1** (1.77 g, 5.08 mmol) in THF (10 mL) was added 6 N KOH (6.68 ml, 40.1 mmol) and the reaction mixture was stirred at room temperature for 12 h [21]. The solution was concentrated and the residue was extracted with chloroform and water. The organic layer was dried over anhydrous Na_2SO_4 and concentrated to give a yellow solid. The crude product was purified by silica gel column chromatography with hexane to give a white solid **2** (87.6%, 913 mg, 4.45 mmol). ^{1}H NMR (300 MHz, $CDCl_3$): δ (ppm) = 3.13 (*s*, 2H, CH), 7.52 (*t*, 1H, $J = 1.5$ Hz, Ar-H), 7.60 (*d*, 2H, $J = 1.5$ Hz, Ar-H).

3,5-Bis(dimethylpentylsilylethynyl)bromobenzene B5. Under nitrogen, bromoethane (1.64 g, 15.0 mmol) was added to magnesium (401 mg, 16.5 mmol) in dry THF (40 mL) and stirred at room temperature for 2 h. Magnesium ethylbromide was added drop wise to the solution of **2** (913 mg, 4.45 mmol) in dry THF (40 mL) for 15 min. After stirring at room temperature for 1 h, dimethylpentylsilylchloride (1.83 g, 11.4 mmol) was added and the reaction mixture was refluxed for 12 h. The reaction was quenched with 1 N HCl and the solution was concentrated. The residue was extracted with hexane and water. The organic layer was dried over anhydrous Na_2SO_4 and concentrated to give a yellow liquid. The crude product was purified by silica gel column chromatography with hexane to give a colorless liquid **B5** (66.1%, 1.36 g, 2.94 mmol). ^{1}H NMR (300 MHz, $CDCl_3$): δ (ppm) = 0.170 (*s*, 12H, CH_3), 0.635 (*t*, 4H, $J = 8.1$ Hz, CH_2), 0.867 (*t*, 6H, $J = 6.8$ Hz, CH_3), 1.29–1.38 (*m*, 12H, CH_2), 7.44 (*t*, 1H, $J = 1.5$ Hz, Ar-H), 7.49 (*d*, 2H, $J = 1.5$ Hz, Ar-H).

Other **Bn** (n = 6–8) were prepared following the same procedure as **B5**.

3,5-Bis(dimethylhexylsilylethynyl)bromobenzene B6. Yield: 65.4%. ^{1}H NMR (300 MHz, $CDCl_3$): δ (ppm) = 0.200 (*s*, 12H, CH_3), 0.675 (*t*, 4H, $J = 7.9$ Hz, CH_2), 0.893 (*t*, 6H, $J = 6.8$ Hz, CH_3), 1.30–1.37 (*m*, 16H, CH_2), 7.47 (*t*, 1H, $J = 1.5$ Hz, Ar-H), 7.53 (*d*, 2H, $J = 1.5$ Hz, Ar-H).

3,5-Bis(dimethylheptylsilylethynyl)bromobenzene B7. Yield: 70.1%. ^{1}H NMR (300 MHz, $CDCl_3$): δ (ppm) = 0.200 (*s*, 12H, CH_3), 0.671 (*t*, 4H, $J = 7.9$ Hz, CH_2),

0.887 (*t*, 6H, $J = 6.8$ Hz, CH_3), 1.28–1.37 (*m*, 20H, CH_2), 7.47 (*t*, 1H, $J = 1.5$ Hz, Ar-H), 7.53 (*d*, 2H, $J = 1.5$ Hz, Ar-H).

3,5-Bis(dimethyloctylsilylethynyl)bromobenzene B8. Yield: 45.3%. ^{1}H NMR (300 MHz, $CDCl_3$): δ (ppm) = 0.200 (*s*, 12H, CH_3), 0.671 (*t*, 4H, $J = 7.9$ Hz, CH_2), 0.881 (*t*, 6H, $J = 6.7$ Hz, CH_3), 1.28–1.37 (*m*, 24H, CH_2), 7.47 (*t*, 1H, $J = 1.4$ Hz, Ar-H), 7.53 (*d*, 2H, $J = 1.4$ Hz, Ar-H).

1,3,6,8-Tetrakis(trimethylsilylethynyl)pyrene 3. Under nitrogen, $PdCl_2(PPh_3)_2$ (83.5 mg, 0.12 mmol), PPh_3 (62.4 mg, 0.24 mmol), *i*-Pr_2NH (15 mL), TMSA (2.34 g, 23.8 mmol), and CuI (22.7 mg, 0.12 mmol) were added to 1,3,6,8-tetrabromopyrene (1.23 g, 2.38 mmol) in dry THF (70 mL). After stirring at 50°C for 20 h, the reaction mixture was cooled to room temperature and filtered through Celite. The filtrate was concentrated and extracted with $CHCl_3$ and water. The organic layer was dried over anhydrous Na_2SO_4 and concentrated to give a reddish-yellow solid. The crude product was purified by silica gel column chromatography with hexane to give a red solid **3** (91.3%, 1.28 g, 2.17 mmol). ^{1}H NMR (300 MHz, $CDCl_3$): δ (ppm) = 0.383 (*s*, 36H, CH_3), 8.31 (*s*, 2H, H^2 and H^7), 8.60 (*s*, 4H, H^4, H^5, H^9, H^{10}).

1,3,6,8-Tetraethynylpyrene 4 [22]. To the solution of **3** (720 mg, 1.23 mmol) in THF (20 mL) was added 6 N KOH 25 mL (150 mmol) and the reaction mixture was stirred at room temperature for 12 h. The solution was concentrated and the residue was washed with chloroform and water to give a yellow solid **4** (97.6%, 358 mg, 1.20 mmol). ^{1}H NMR (300 MHz, DMSO-d_6): δ (ppm) = 5.01 (*s*, 4H, CH), 8.43 (*s*, 2H, H^2 and H^7), 8.70 (*s*, 4H, H^4, H^5, H^9, H^{10}).

1,3,6,8-Tetrakis[3,5-bis(dimethylpentylsilylethynyl)phenylethynyl]pyrene A5 [21,22]. Under nitrogen, $PdCl_2(PPh_3)_2$ (11.9 mg, 0.0170 mmol), PPh_3 (8.9 mg, 0.034 mmol), *i*-Pr_2NH (20 mL), **B5** (630 mg, 1.37 mmol), and CuI (3.2 mg, 0.017 mmol) were added to **4** (102 mg, 0.342 mmol) in dry toluene (40 mL). After stirring at 50°C for 48 h, the reaction mixture was cooled to room temperature and filtered through Celite. The filtrate was concentrated and extracted with chloroform and water. The organic layer was dried over anhydrous Na_2SO_4 and concentrated to give a red liquid. The crude product was purified by silica gel column chromatography with hexane, by TLC on silica gel with hexane, and by molecular sieve chromatography with hexane. The eluent was concentrated and washed with acetone to afford **A5** as an orange solid (26.2%, 163 mg, 0.0896 mmol). mp: 122.0–123.6°C. ^{1}H NMR (400 MHz, $CDCl_3$): δ (ppm) = 0.251 (*s*, 48H, CH_3), 0.713 (*t*, 16H, $J = 8.0$ Hz, CH_2), 0.924 (*t*, 24H, $J = 7.0$ Hz, CH_3), 1.36–1.47 (*m*, 48H, CH_2), 7.60 (*t*, 4H, $J = 1.5$ Hz, Ar-H), 7.75 (*d*, 8H, $J = 1.5$ Hz, Ar-H), 8.41 (*s*, 2H, H^2 and H^7), 8.74 (*s*, 4H, H^4, H^5, H^9, H^{10}). MALDI-TOF MS *m/z* (%): Anal. Calc. for $C_{120}H_{154}Si_8$ 1819.0199; Found: 1819.0189 (M^+, 43%), 1820.0329 (100%), 1821.0388 (99%), 1822.0384 (72%), 1823.0393 (34%), 1824.0394 (10%). Anal. Calc. for $C_{120}H_{154}Si_8$: C, 79.14; H, 8.52. Found: C, 78.83; H, 8.56.

Other **An** (n = 6–8) were prepared following the same procedure as **A5**.

1,3,6,8-Tetrakis[3,5-bis(dimethylhexylsilylethynyl)phenylethynyl]pyrene A6. Yield: 8.1%. mp: 110.1–112.1°C. ^{1}H NMR (300 MHz, $CDCl_3$): δ (ppm) = 0.243 (*s*, 48H, CH_3), 0.715 (*t*, 16H, $J = 7.9$ Hz, CH_2), 0.905 (*t*, 24H, $J = 6.8$ Hz, CH_3), 1.26–1.41 (*m*, 64H, CH_2), 7.60 (*t*, 4H, $J = 1.5$ Hz, Ar-H), 7.75 (*d*, 8H, $J = 1.5$ Hz, Ar-H), 8.41 (*s*, 2H, H^2 and H^7), 8.75 (*s*, 4H, H^4, H^5, H^9, H^{10}). MALDI-TOF MS *m/z*

(%): Anal. Calc. for $C_{128}H_{170}Si_8$ 1931.1451; Found: 1931.1444 (M^+, 36%), 1932.1379 (86%), 1933.1315 (100%), 1934.1253 (71%), 1935.1193 (33%), 1936.1512 (13%). Anal. Calc. for $C_{128}H_{170}Si_8$: C, 79.52; H, 8.86. Found: C, 79.40; H, 8.91.

1,3,6,8-Tetrakis[3,5-bis(dimethylheptylsilylethynyl)phenylethynyl]pyrene A7. Yield: 10.1%. mp: 90.4–91.4°C. ^{1}H NMR (300 MHz, $CDCl_3$): δ (ppm) = 0.241 (*s*, 48H, CH_3), 0.711 (*t*, 16H, $J = 7.9$ Hz, CH_2), 0.888 (*t*, 24H, $J = 6.8$ Hz, CH_3), 1.26–1.42 (*m*, 80H, CH_2), 7.60 (*t*, 4H, $J = 1.8$ Hz, Ar-H), 7.75 (*d*, 8H, $J = 1.8$ Hz, Ar-H), 8.41 (*s*, 2H, H^2 and H^7), 8.75 (*s*, 4H, H^4, H^5, H^9, H^{10}). MALDI-TOF MS *m/z* (%): Anal. Calc. for $C_{136}H_{186}Si_8$ 2043.2703; Found: 2043.2664 (M^+, 42%), 2044.2481 (89%), 2045.2702 (100%), 2046.2532 (78%), 2047.2758 (45%), 2048.2637 (19%), 2049.2809 (7%). Anal. Calc. for $C_{136}H_{186}Si_8$: C, 79.85; H, 9.17. Found: C, 78.90; H, 9.29.

1,3,6,8-Tetrakis[3,5-bis(dimethyloctylsilylethynyl)phenylethynyl]pyrene A8. Yield: 19.3%. mp: 48.8 – 52.7°C. ^{1}H NMR (400 MHz, $CDCl_3$): δ (ppm) = 0.243 (*s*, 48H, CH_3), 0.710 (*t*, 16H, $J = 8.0$ Hz, CH_2), 0.870 (*t*, 24H, $J = 6.8$ Hz, CH_3), 1.28–1.43 (*m*, 96H, CH_2), 7.60 (*t*, 4H, $J = 1.6$ Hz, Ar-H), 7.75 (*d*, 8H, $J = 1.6$ Hz, Ar-H), 8.41 (*s*, 2H, H^2 and H^7), 8.75 (*s*, 4H, H^4, H^5, H^9, H^{10}). MALDI-TOF MS *m/z* (%): Anal. Calc. for $C_{144}H_{202}Si_8$ 2155.955; Found: 2155.3926 (M^+, 31%), 2156.3985 (85%), 2157.3997 (100%), 2158.4047 (79%), 2159.3972 (44%), 2160.3953 (19%), 2161.3989 (6%). Anal. Calc. for $C_{144}H_{202}Si_8$: C, 80.15; H, 9.44. Found: C, 80.27; H, 9.71.

Results and Discussion

Synthesis

To prepare highly conjugated pyrene derivatives, phenylacetylene moieties were introduced onto the pyrene core not only to increase π-conjugation but also to reduce the steric hindrance of the trialkylsilyl groups (Scheme 1). As a result, a novel class of pyrene derivatives, **An** (n = 5–8), was designed and synthesized in a

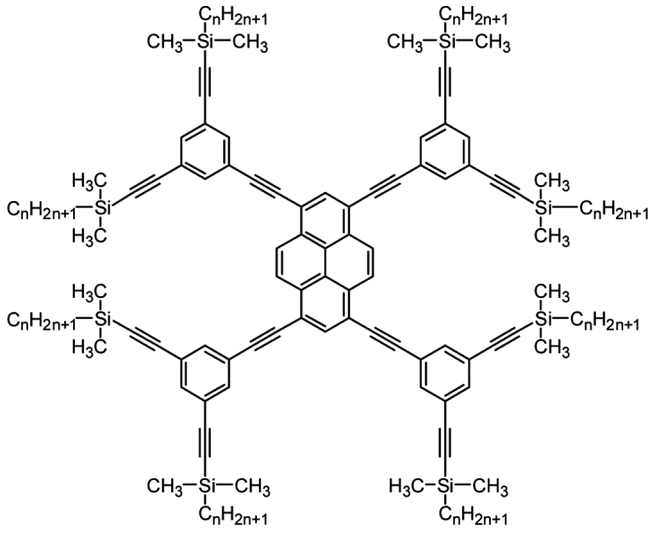

Scheme 1. 1,3,6,8-Tetrakis[3,5-bis(dimethylalkylsilylethynyl)phenylethynyl]pyrene **An**.

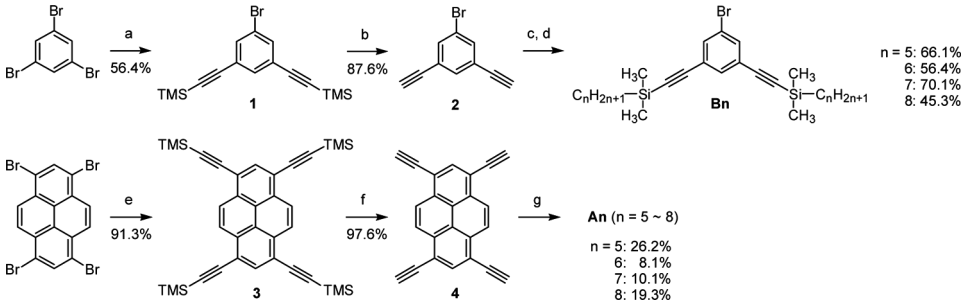

Scheme 2. Synthetic route of 1,3,6,8-tetrakis[3,5-bis(dimethylalkylsilylethynyl)phenylethynyl]-pyrene **An**. (a) 2 *eq.* TMSA, *cat.* $PdCl_2(PPh_3)_2$, *cat.* CuI, *cat.* PPh_3/dry THF-*i*-Pr_2NH, 50°C, 20 h; (b) 6 N KOH aq./THF, rt, 12 h; (c) C_2H_5MgBr/dry THF, rt, 1 h; (d) 2 *eq.* $ClSi(CH_3)_2C_nH_{2n+1}$/dry THF, reflux, 12 h; (e) 4 *eq.* TMSA, *cat.* $PdCl_2(PPh_3)_2$, *cat.* CuI, *cat.* PPh_3/dry THF-*i*-Pr_2NH, 50°C, 20 h; (f) 6 N KOH aq./THF, rt, 12 h; (g) 4 *eq.* **Bn** (n = 5–8), *cat.* $PdCl_2(PPh_3)_2$, *cat.* CuI, *cat.* PPh_3/dry toluene-*i*-Pr_2NH, 50°C, 48 h. TMSA = trimethylsilylacetylene.

straightforward manner, as shown in Scheme 2. The total yield was between 7% for **A6** and 23% for **A5** starting from 1,3,6,8-tetrabromopyrene and 3,5-bis(alkyldimethylsilylethynyl)bromobenzene, respectively, which were prepared in 45% (**R8**) to 70% (**R7**) yield from 1,3,5-tribromobenzene. The yield of the last step, Sonogashira coupling, strongly depends on the reaction conditions and requires further optimization. All **An** (n = 5–8) were soluble in $CHCl_3$, toluene, and even hexane and were purified by repeated chromatography using hexane. The high solubility of these compounds in common organic solvents arises from the eight alkyldimethylsilyl groups as well as the small pyrene core.

Thermal and UV-Vis Absorption Properties

The thermal behavior of the compounds was investigated by DSC and POM, and **A5** and **A6** were found to exhibit liquid-crystalline phases (Table 1). The mesophases

Table 1. Phase transition behavior of **An**

	Phase transition temperatures (°C) and enthalpy changes (kJ/mol)	
Compound	Heating	Cooling
A5	Cr_1 105 (8.8) Cr_2 116 (2.4) **Col_r** 150 (6.8) I	I 144 (7.1) **Col_r** 89 (7.1) Cr
A6	Cr 86 (12.1) **Col_r** 114 (6.1) I	I 105 (7.1) **Col_r** 69 (10.5) Cr
A7	Cr_1 41 (3.5) Cr_2 72 (14.3) Cr_3 88 (10.8) I	I 53 (4.7) Cr_4 31 (2.6) Cr_5
A8	Cr 41 (9.3) I	—[a]

Transition temperatures were determined by DSC. Scan rate was 5°C/min.

Abbreviations: Cr = crystalline phase; I = isotropic phase; Col_r = rectangular columnar phase.

[a]Not crystallized during the DSC measurement.

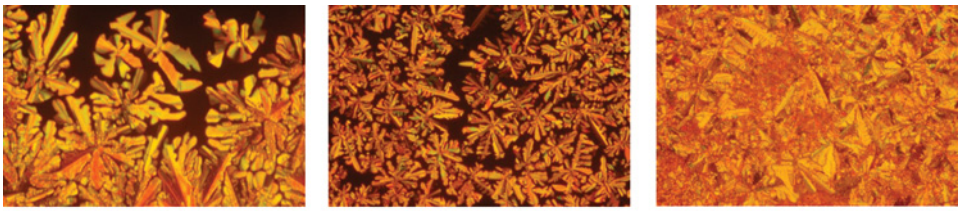

Figure 1. Optical textures of (a) **A5** at 140°C, (b) **A6** at 100°C, and (c) **A6** at 60°C during the cooling process.

obtained upon cooling of their isotropic phases displayed dendritic textures (Figs. 1a and 1b) characteristic of a Col_r phase. On the other hand, **A7** and **A8** were crystalline as observed by POM and showed only melting behavior.

The structures of **A5** and **A6** in the mesophases were investigated by XRD analysis. The diffraction pattern of **A5** at 120°C during the cooling process is shown in Fig. 2. Two sharp peaks were observed at 24.7 and 22.9 Å, and small ones at 10.2, 9.4, 8.7, 8.4, 8.0, and 7.6 Å were observed. A broad halo and a faint shoulder were observed in the wide-angle region corresponding to the molten chains (h_{ch} at 5.0 Å) and to the stacking of the molecular cores (h at 3.6 Å), respectively. These reflection patterns are indicative of a liquid-crystalline phase in this temperature range. Although these were assigned to neither a simple lamellar nor hexagonal structure, the two sharp peaks in the small-angle region suggested a rectangular structure (Col_r). Based on the assumption that the two intense peaks were (110) and (200) reflections, respectively, other peaks could be indexed as (230), (420), (510), (140), (240), and (600). In the same manner, the structure of **A6** was assigned as Col_r, and the results for **A5** and **A6** are summarized in Table 2.

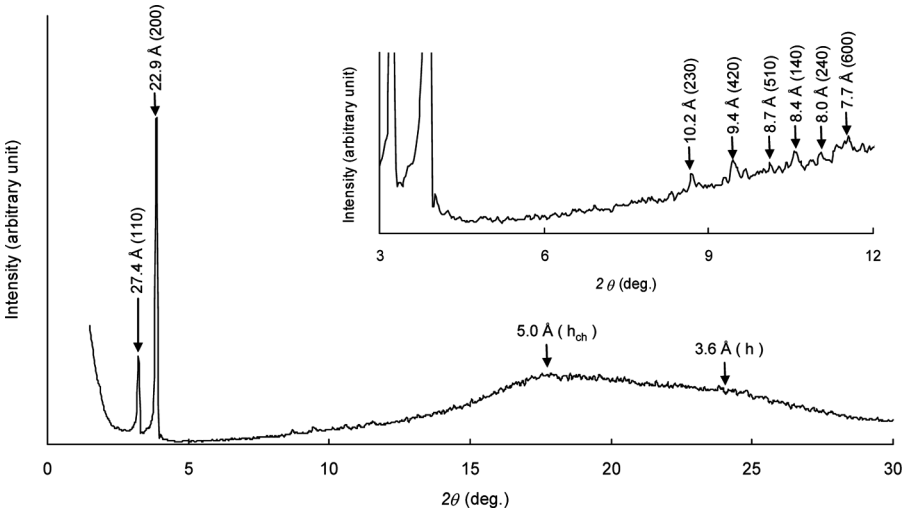

Figure 2. X-ray diffraction pattern of **A5** at 120°C during the cooling process.

Table 2. X-ray diffraction data of **A5** (120°C) on the cooling process and **A6** (85°C) on the heating process

Compound	Phase	Lattice constant (Å)	Spacing (Å)		Miller indices (h k l)
			d_{obs}	d_{calc}	
A5	Col_r	$a = 45.8$	27.4	27.4	110
120°C	P2i/a	$b = 34.1$	22.9	22.9	200
		$Z = 2$	10.2	10.2	230
			9.4	9.5	420
			8.7	8.9	510
			8.4	8.4	140
			8.0	8.0	240
			7.6	7.6	600
			6.9	7.0	620
			6.7	6.8	150
			6.4	6.3	630
			6.1	6.1	720
			5.9	5.9	450
			5.0		h_{ch}
			3.6		h
A6	Col_r	$a = 47.7$	27.8	27.9	110
85°C	$P2_x/a$	$b = 34.4$	23.6	23.9	200
		$Z = 2$	19.7	19.6	210
			10.2	10.3	230
			9.5	9.3	330
			8.6	8.6	040
			8.0	8.0	600
			5.0		h_{ch}
			3.7		H

$Z = (\rho \cdot a \cdot b \cdot h \cdot N_A)/M$. Z = Molecular numbers per unit cell, N_A = Avogadro's number, a and b = lattice constant, h = stacking distance, ρ = density (assumed to be $1.0\,g\,cm^{-3}$), M = molecular weight of the compound.

The UV-Vis absorption spectrum of **A5** in hexane features absorption in the range of 380–480 nm, which is in the visible light region (Fig. 3). Substitution of the pyrene core with ethynyl and phenyl groups contributed to a large red-shift of the lowest absorption by ~130 nm, which resulted in an orange color [18].

Hole Transport Properties

The positive charge (hole) photocurrents were measured as a function of time over the temperature range of the Col_r and Cr phases by the TOF method (Fig. 4 for **A5**). The hole mobility was confirmed to be bias independent for both phases of each sample, as shown for **A5** at 125°C in Fig. 5. On the other hand, in the isotropic phase, negligible charge mobility was observed, probably due to the decrease of π-π stacking in the isotropic state. The results were analyzed in double logarithmic plots as shown in the inset of Fig. 4 at 135°C, 125°C (Col_r), and 75°C (Cr) because

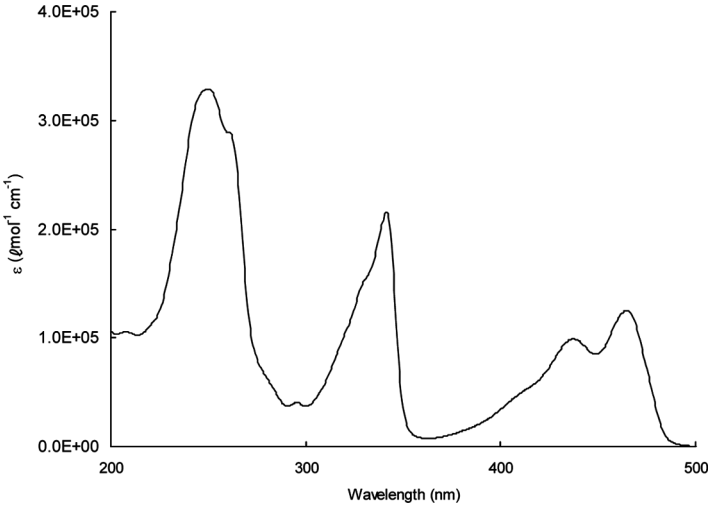

Figure 3. UV-Vis spectrum of **A6** (1.0×10^{-5} mol/L) in n-C_6H_{14}.

the raw data in the Cr phase were dispersive, which was attributed to disruption in molecular alignment at the grain boundaries during crystallisation and trapping of charge carriers. The intercept of the two lines corresponding to the pre- and post-stransit slopes gave the transit time, τ_T.

The results for hole mobility as a function of temperature are shown for **A5** and **A6** in Fig. 6. It was found that the hole transport in the columnar phase slightly decreases as temperature decreases. On the other hand, upon cooling from the Col_r to the Cr phases, hole mobility was observed to decrease by factor of ~2 for **A5** and

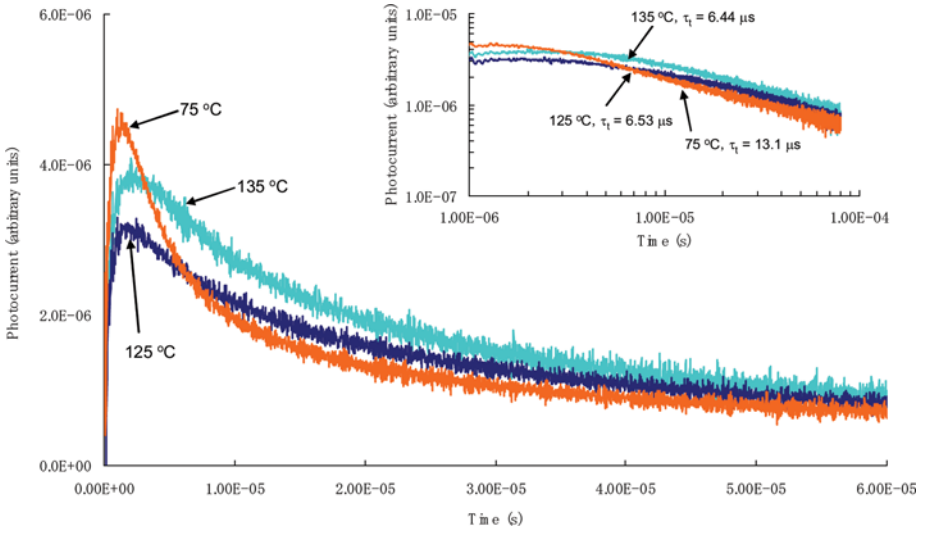

Figure 4. Typical transient photocurrents for the hole mobility during the cooling process of **A5** in an electric field of 5.0 kV cm^{-1} at 135°C, 125°C, and 75°C. The inset shows the double logarithmic plots. The cell thickness was 5.0 μm.

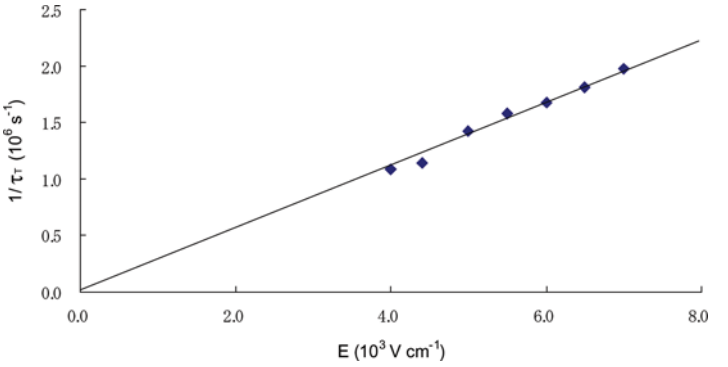

Figure 5. Electric field dependence of hole mobility for **A5** at 125°C. The cell thickness was 5.0 μm. $R^2 = 0.9849$.

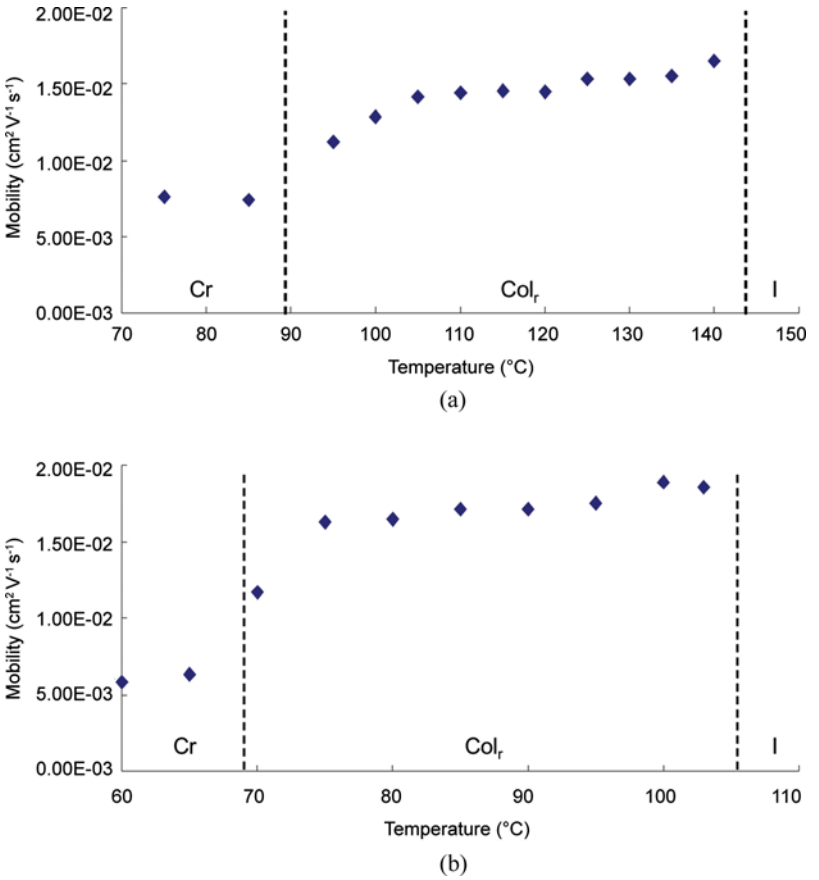

Figure 6. Temperature dependence of hole mobilities for (a) **A5** and (b) **A6** during the cooling processes. The data were collected at 75°C–140°C for **A5** and at 60°C–103°C for **A6**. The electric field was 5.0 kV cm^{-1} and the cell thickness was 5.0 μm for both **A5** and **A6**.

$\sim$3 for **A6** around the transition. These decreases can be understood from the texture changes shown in Figs. 1b and 1c for **A6**; specifically, because some columnar liquid crystals exhibit higher mobility in the crystalline phases [23] or super cooled state [24], some columnar structure was considered to remain. For other discotic liquid crystals, similar decreases in the hole mobility at the Col to Cr phase transition have been observed [25–27]. In the present system, the bulky trialkylsilyl groups might have disturbed the molecular alignment and the intermolecular interactions.

The hole mobilities of **A5** and **A6** were found to be on the order of $10^{-2}\,cm^2\,V^{-1}\,s^{-1}$ in the liquid-crystalline phase and $10^{-3}\,cm^2\,V^{-1}\,s^{-1}$ in the crystalline phase. The values for the mesophases are rather high in comparison with other discotic liquid-crystalline compounds, especially considering that both samples are pyrene derivatives and in the Col_r phase [23–30]. The transport ability is thought to arise from the highly conjugated system with σ-π conjugation of the terminal trialkylsilylethynyl groups. To the best of our knowledge, **A5** and **A6** are the first discotic liquid crystals bearing trialkylsilyl groups and exhibit the highest reported hole mobilities among pyrene derivatives determined by the TOF method.

Conclusions

Highly soluble pyrene derivatives were prepared by introduction of trialkylsilylethynyl groups with phenylacetylene moieties. TOF measurements indicated that the hole transport abilities in the Col_r phase for two compounds, **A5** and **A6**, are on the order of $10^{-2}\,cm^2\,V^{-1}\,s^{-1}$ and two to three times higher than their hole transport abilities in the Cr phase. These hole mobilities, which are the highest yet observed for pyrene derivatives in the mesophase determined by the TOF method [29,30], and the transport characteristics of these compounds are thought to arise from unique σ-π conjugation properties and the bulkiness of the trialkylsilyl groups in the conjugated side chains.

References

[1] Tang, C. W., & VanSlyke, S. A. (1987). *Appl. Phys. Lett.*, *51*, 913.
[2] Kunugi, Y., Takimiya, K., Yamashita, K., Aso, Y., & Otsubo, T. (2002). *Chem. Lett.*, *31*, 958.
[3] O'Neil, M., & Kelly, S. M. (2003). *Adv. Mater.*, *15*, 1135.
[4] Jurchescu, O. D., Popinciuc, M., van Wees, B. J., & Palstra, T. T. M. (2007). *Adv. Mater.*, *19*, 688.
[5] (a) Inoue, T., Yase, K., Inaoka, K., & Okada, M. (1987). *J. Cryst. Growth*, *83*, 306; (b) Tanaka, K., Umemoto, S., Okui, N., & Sakai, T. (1991). *Thin Solid Films*, *196*, 137.
[6] Van der Auweraer, M., De Schryver, F. C., Borsenberger, P. M., & Bässler, H. (1994). *Adv. Mater.*, *6*, 199.
[7] (a) Hanna, J. (2007). *Opto-Electronics Review*, *13*, 295–302; (b) Zhang, F., Funahashi, M., & Tamaoki, N. (2007). *Appl. Phys. Lett.*, *91*, 063515.
[8] Funahashi, M., Zhang, F., & Tamaoki, N. (2007). *Adv. Mater.*, *19*, 353.
[9] Pisula, W., Menon, A., Stepputant, M., Lieberwirth, I., Kolb, U., Tracz, A., Sirringhaus, H., Pakula, T., & Mullen, K. (2005). *Adv. Mater.*, *17*, 684.
[10] Bushby, R. J., & Lozman, O. R. (2002). *Curr. Opin. Solid State Mater. Sci.*, *6*, 569.
[11] (a) Iino, H., Takayashiki, Y., Hanna, J., & Bushby, R. J. (2005). *Jpn. J. Appl. Phys.*, *44*, L1310; (b) Iino, H., Hanna, R. J., Bushby, J., Movaghar, B., Whitaker, B. J., & Cook, M. J. (2005). *Appl. Phys. Lett.*, *87*, 132102.

[12] Zhang, H., Wang, Y., Shao, K., Liu, Y., Chen, S., Qiu, W., Sun, X., Qi, T., Ma, Y., Yu, G., Su, Z., & Zhu, D. (2006). *Chem. Comm.*, 755.
[13] van Breemen, A. J. J. M., Herwig, P. T., Chlon, C. H. T., Sweelssen, J., Schoo, H. F. M., Setayesh, S., Hardeman, W. M., Martin, C. A., de Leeuw, D. M., Valeton, J. J. P., Bastiaansen, C. W. M., Broer, D. J., Popa-Merticaru, S. C. J., & Meskers, A. R. (2006). *J. Am. Chem. Soc.*, *128*, 2336.
[14] (a) Yasutake, M., Fujihara, T., Nagasawa, A., Moriya, K., & Hirose, T. (2008). *Eur. J. Org. Chem.*, 4120; (b) Hirose, O., Kawakami, T., & Yasutake, M. (2006). *Mol. Cryst. Liq. Cryst.*, *451*, 1563.
[15] Ohshita, J., Lee, K. H., Hashimoto, M., Kunugi, Y., Harima, Y., Yamashita, K., & Kunai, Y. (2002). *Org. Lett.*, *4*, 1891.
[16] Yamaguchi, S., & Tamao, K. (1996). *Bull. Chem. Soc. Jpn.*, *69*, 2327.
[17] Karatsu, T., Shibata, T., Nishigaku, A., Fukui, K., & Kitamura, A. (2001). *Chem. Lett.*, *30*, 994.
[18] (a) Maeda, H., Inoue, Y., Ishida, H., & Mizuno, K. (2001). *Chem. Lett.*, *30*, 1224; (b) Maeda, H., Maeda, T., Mizuno, K., Fujimoto, K., Shimizu, H., & Inouye, M. (2006). *Chem. Eur. J.*, *12*, 824.
[19] (a) Chen, Z.-K., Wang, L.-H., Kang, E.-T., Lai, Y.-H., & Huang, W. (1999). *Bul. Chem. Soc. Jpn.*, *72*, 1941; (b) Chen, Z.-K., Huang, W., Wang, L.-H., Kang, E.-T., Chen, B. J., Lee, C. S., & Lee, S. T. (2000). *Macromolecules*, *33*, 9015.
[20] Okumoto, H., Yatabe, T., Shimomura, M., Kaito, A., Minami, N., & Tanabe, Y. (2001). *Adv. Mater.*, *13*, 72.
[21] Suresh, P., Srimurugan, S., Babu, B., & Pati, H. N. (2007). *Tetrahedron: Asymmetry*, *18*, 2820.
[22] Hayer, A., de Halleux, V., Kölhler, A., El-Garoughy, A., Meijer, E. W., Barberá, J., Tant, J., Levin, J., Lehmann, M., Gierschner, J., Cornil, J., & Geerts, Y. H. (2006). *J. Phys. Chem. B*, *110*, 7653.
[23] (a) van de Craats, A. M., Warman, J. M., Fechtenkötter, A., Brand, J. D., Harbison, M. A., & Müllen, K. (1999). *Adv. Mater.*, *11*, 1469; (b) Debije, M. G., Piris, J., de Haas, M. P., Warman, J. M., Tomović, Ž., Simpson, M. D., Watson, C. D., & Müllen, K. (2004). *J. Am. Chem. Soc.*, *126*, 4641.
[24] Adam, D., Schuhmacher, P., Simmerer, J., Häussling, L., Siemensmeyer, K., Etzbach, K. H., Ringsdorf, D., & Haarer, H. (1994). *Nature*, *371*, 141.
[25] Adam, D., Römhildt, W., & Haarer, D. (1996). *Jpn. J. Appl. Phys.*, *35*, 1826.
[26] Yoshimo, K., Nakayama, H., Ozaki, M., Onoda, M., & Hamaguchi, M. (1997). *Jpn. J. Appl. Phys.*, *36*, 5183.
[27] Yasuda, T., Ooi, H., Morita, J., Akama, Y., Minoura, K., Funahashi, M., Shimomura, T., & Kato, T. (2008). *Adv. Funct. Mater.*, *18*, 1.
[28] Iino, H., Takayashiki, Y., Hanna, J., Bushby, R. J., & Haarer, D. (2005). *Appl. Phys. Lett.*, *87*, 192105.
[29] Sienkowska, M. J., Monobe, H., Kaszynski, P., & Shimizu, Y. (2007). *J. Mater. Chem.*, *17*, 1392.
[30] Shiyanovskaya, I., Singer, K. D., Percec, V., Bera, T. K., Miura, Y., & Glodde, M. (2003). *Phys. Rev. B*, *67*, 035204.